

CONTRIBUTOR'S ABSTRACTS

1st day

Yasuji OURA¹, Takayuki NAGAMINE¹, Shigekazu YONEDA², Mitsuru EBIHARA¹, and Masatake HONDA¹

¹ Department of Chemistry, Graduate School of Science, Tokyo Metropolitan University, Hachioji-shi, Tokyo 192-0397, Japan

² The National Science Museum, Shinjuku-ku, Tokyo, 169-0073, Japan

^{53}Mn is an extinct nuclide and exists in meteorites as a cosmogenic nuclide produced mainly via a spallation reaction of Fe. In cosmochemical study, ^{53}Mn has been used to obtain cosmic-ray-exposure age of meteorites. Recently, with developing the technique on mass spectrometry, ^{53}Mn - ^{53}Cr chronology has become popular to study an early stage chronology of the solar system. ^{53}Mn will play more important role in cosmochemistry in future.

The half life of ^{53}Mn used presently is 3.7×10^6 years, which was reported in 1971¹. Because of the long half life, the half life of ^{53}Mn cannot be determined by following a decay. Therefore, it is calculated from a number of atoms and an absolute activity. Electron capture decaying ^{53}Mn does not release γ -rays but emits only characteristic X-rays of decayed (daughter) element, Cr (5.4 keV for K_{α}). So, it is not easy to determine its absolute activity. Honda *et al.*¹ used a neutron activation method to determine an absolute activity of ^{53}Mn in the sample instead of X-ray measurement. No values of the half life of ^{53}Mn have not been reported since 1971.

We started re-measuring the half life of ^{53}Mn with higher accuracy and precision using a developed radiation detector and a mass spectrometer, with determining directly an absolute activity of ^{53}Mn by X-ray counting. The chemical separation scheme for Mn, X-ray measurement, and mass spectrometry were partly presented at SORC-44 last year². Based on these results, ^{53}Mn was chemically separated from 56 g of Canyon Diablo iron meteorite. Then X-ray measurement and mass spectrometry were performed. Though 24 μg of Mn was separated from the meteorite, neither X-ray nor ^{53}Mn beam were detected. It was concluded that those results were caused by very low ^{53}Mn content in our specimen of Canyon Diablo used. The ^{53}Mn content in the remaining Canyon Diablo specimen was found to be < 3.5 dpm ^{53}Mn /kg Fe, although much higher contents (250 dpm ^{53}Mn /kg Fe) was reported for other specimens of this meteorite. It was confirmed that Mn was sufficiently separated from Cr, one of which isotope, ^{53}Cr , interferes ^{53}Mn in mass spectrometry. It was also observed that the presence of excess Fe disarranges an elution of Mn from an anion exchange resin column. With reference to results for Canyon Diablo, newly prepared of ^{53}Mn sample from 56 g of ALH77250 iron meteorite is in progress.

1. M.Honda, M.Imamura, *Phys.Rev.***4**, 1182 (1971).

2. T.Nagamine, Y.Oura, S.Yoneda, M.Ebihara, M.Honda, *SORK-44*, 23 (2000).

1A2 AN ATTEMPT TO CHANGE THE HALF- LIVES OF β -DECAY NUCLIDES

Naruto TAKAHASHI¹, Hiroshi BABA², Atsushi SHINOHARA¹, Akihiko YOKOYAMA³,
Atsushi TOYOSHIMA¹, Yoshitaka KASAMATSU¹, Kunio GOTO¹, Yuzuru SHOJI¹,
Tomoyuki KOIKE¹ and Koichi TAKAMIYA⁴

¹Graduate School of Science, Osaka University, Toyonaka Osaka 650-0043, Japan

²Radioisotope Research Center, Osaka University, Suita Osaka 565-0871, Japan

³Faculty of Science, Kanazawa University, Kanazawa 920-1192, Japan

⁴Research Reactor Institute, Kyoto University, Kumatori Osaka 590-0494, Japan

It has been believed that the half-lives of radioisotopes can't be changed by changing the physical or chemical condition except for the ultrahigh temperature and pressure surroundings occurred inside of the stars. The reason is that the half-life is a well defined physical constant which can't be affected by human beings with an ordinary means.

According to Fermi's β -decay theory¹, the life time of a β -decay nuclide is inversely proportional to the electron density at the position of the nucleus. It was attempted to change the half-lives of β -decay nuclides by stripping orbital electrons by means of X-ray irradiation at the BL08W line of SPring-8. β -decay nuclides were prepared by neutron irradiation using Kyoto University reactor KUR. La-140 and ¹⁹⁸Au were chosen as activities to be studied.

The ¹⁴⁰La, ¹⁹⁸Au and ¹³⁷Cs used as monitor were irradiated by synchrotron radiation at 115 keV BL08W beam line for 12 shifts, 96 hours. Gamma rays and X-rays from the samples were measured with two Ge detectors, respectively. Signals from the Ge detectors were fed into the multi-channel pulse height analyzers to construct the γ -ray and X-ray spectra. The obtained spectra were analyzed using a spectrum analyzing program BOB76.

Time sequences of photopeak intensities of typical γ -rays from ¹⁴⁰La and ¹⁹⁸Au were obtained. Although the activities of the sample were traced through 80 hours, abnormal half-lives were observed only for early part of the decay (14 hours). The deduced half-life values are 39.30 ± 0.28 hours and 60.49 ± 0.27 hours for ¹⁴⁰La and ¹⁹⁸Au, respectively.

The obtained half-lives are 3~5% smaller than the literature values as obtained in the preliminary work. On the other hand, the half-lives obtained by using all data for 82 hours agreed very well with the reported values of ¹⁴⁰La and ¹⁹⁸Au.

1. E. Fermi, *Z. Phys.*, **85**,161(1934).

Toshiaki MITSUGASHIRA¹, Mitsuo HARA¹, Tsutomu OHTSUKI², Hideyuki YUKI²,
Koichi TAKAMIYA³, Yoshitaka KASAMATSU⁴, Atsushi SHINOHARA⁴,
Hidetoshi KIKUNAGA⁵, Takashi NAKANISHI⁶

¹The Oarai-branch, IMR, Tohoku University, Oarai-machi, Ibaraki 311-1313, Japan

²LNS, Graduate School of Science, Tohoku University, Sendai 982-0826, Japan

³Research Reactor Institute, Kyoto University, Kumatori, Osaka 590-0494, Japan

⁴Graduate School of Science, Osaka University, Toyonaka, Osaka 560-0043, Japan

⁵Graduate School of Nat. Sci. Tech., Kanazawa University, Kanazawa 920-1192, Japan

⁶Faculty of Science, Kanazawa University, Kanazawa 920-1192, Japan

The excitation energy of the $3/2^+$ [631] level of $^{229\text{m}}\text{Th}$ was reported to be less than 5 eV and 3.5 eV in $^{230}\text{Th}(d,t)$ scattering and precise γ -ray spectroscopy, respectively. Because the energy is lower than the 1st ionization potential of Th and, thus, the internal conversion is prohibited, $^{229\text{m}}\text{Th}$ mainly decays through a direct γ -transition and the electronic bridge interaction (EBM). This implies that the $t_{1/2}$ of $^{229\text{m}}\text{Th}$ depends on its chemical state that relates to the probability of EBM. Previous attempts to observe direct γ -transition were unsuccessful. We select a different approach to observe the minor α -decay of $^{229\text{m}}\text{Th}$. The most favored α -transition from $^{229\text{m}}\text{Th}$ feeds the 149.96 keV $3/2^+$ [631] level of ^{225}Ra ($E_\alpha = 4.930$ MeV), whereas the ^{229}Th feeds the much higher levels of ^{225}Ra . As a result, the α -particles from $^{229\text{m}}\text{Th}$ have larger energies than those from ^{229}Th and the partial half-life of the α -transition from $^{229\text{m}}\text{Th}$ is considerably shorter than that of ^{229}Th . Instead of the α -decay of ^{233}U , we selected $^{230}\text{Th}(\gamma, n)^{229\text{m}}\text{Th}$ and $^{232}\text{Th}(\gamma, p2n)^{229}\text{Ac}(t_{1/2} = 62.7 \text{ m}) \rightarrow \beta^- \rightarrow ^{229\text{m}}\text{Th}$ reactions to produce $^{229\text{m}}\text{Th}$. The Bremsstrahlung irradiation was carried out using the electron linear accelerator of Tohoku University that was operated at electron energies of 22, 30, and 50 MeV with the mean beam current around 0.1 mA. After the irradiation, the mixture of ^{230}Th , $^{229\text{m}}\text{Th}$, and ^{228}Th was isolated and its α -spectrum was traced. We observed the production of new α -emitter with its half-life of about 15 hours between the α -peaks of ^{230}Th and ^{228}Th . The energy of the decaying component is consistent with that expected for $^{229\text{m}}\text{Th}$.

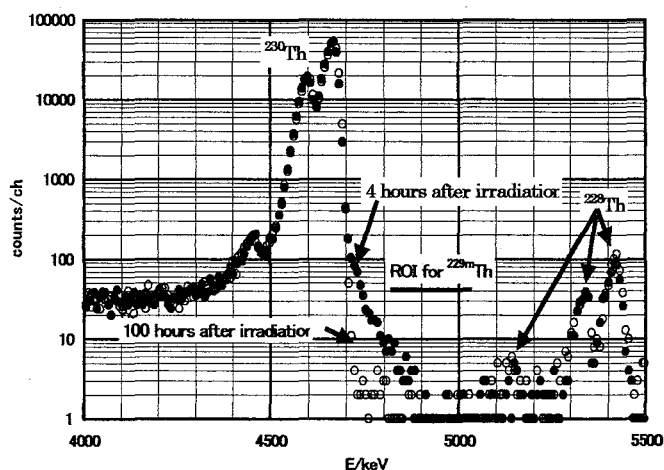


Fig.1 α -spectra of thorium isotopes after 30 MeV Bremsstrahlung irradiation on ^{230}Th target.

S. ICHIKAWA¹, M. ASAI¹, A. OSA¹, K. TSUKADA¹, H. HABA¹, Y. NAGAME¹, S. GOTO²,
M. SHIBATA³, Y. KOJIMA⁴, and M. SAKAMA⁵

¹Japan Atomic Energy Research Institute, Tokai, Ibaraki 319-1195, Japan

²Department of Chemistry, Niigata University, Niigata 950-2181, Japan

³Facility for Nuclear Materials, Nagoya University, Nagoya 464-8603, Japan

⁴Graduate School of Engineering, Hiroshima University, Higashi-Hiroshima 739-8527, Japan

⁵Department of Radiological Technology, University of Tokushima, Tokushima 770-8509, Japan

β^- -decay half-lives are one of the important quantities related to the stability of neutron-rich nuclei as well as to the astrophysical calculations involving the rapid neutron capture process (r-process). Although the nuclei studied up to the present do not directly affect the evaluation of the nuclidic abundance produced in the r-process, their experimental half-lives give a good opportunity to verify the validity of various theoretical calculations of β -decay half-lives. In the previous work, we determined β -decay half-lives of the isotopes ^{161}Sm , ^{165}Gd , and $^{166,167,168}\text{Tb}$ [1,2] produced in the proton-induced fission of ^{238}U , and it was found that the half-life values observed are in good agreement with those predicted from the gross theory. In this report, we present the newly determined half-life values of the three isotopes ^{159}Pm , ^{162}Sm and ^{166}Gd together with that of the re-measured ^{166}Tb .

The experiments were performed at the JAERI (Japan Atomic Energy Research Institute) tandem accelerator facility. A stack of eight ^{238}U targets (4 mg/cm² thick each) was bombarded with a 15.5 MeV proton beam with the intensity of about 3 μA . Fission products recoiling out of the targets were transported into an ion source of the JAERI-ISOL with the He/PbI₂ gas-jet stream. The transported nuclides were ionized and mass-separated as the monoxide ions. The mass-separated products were collected on an aluminized Mylar tape and periodically transported to a measuring position. β - γ and γ - γ coincidence measurements were performed with a sandwich-type plastic scintillator and two HPGe detectors.

The measured half-life values were 1.42 ± 0.15 s for ^{159}Pm , 2.4 ± 0.5 s for ^{162}Sm , 4.8 ± 1.0 s for ^{166}Gd and 25.6 ± 2.2 s for ^{166}Tb , respectively. As one of the nuclear decay properties, γ rays associated with the β^- -decay of each isotopes were also assigned on the basis of x- γ , γ - γ coincidences; for ^{159}Pm , 71.8- and 261.3 keV; for ^{162}Sm , 36.0-, 736.6- and 741.1 keV; and for ^{166}Gd , 40.0-, 118.8-, 158.8-, 536.0-, 975.5- and 1015.5 keV, respectively. In the conference, a detail comparison of the experimental half-life values with the results of two theoretical predictions, and the decay properties of the isotopes studied will be discussed.

[1] S. Ichikawa *et al.*, *Phys. Rev. C* **58**, 1329 (1998).

[2] M. Asai *et al.*, *Phys. Rev. C* **59**, 3060 (1999).

FRAGMENT MASS AND TOTAL KINETIC ENERGY DISTRIBUTIONS IN FISSION OF LIGHT ACTINIDES

Ichiro NISHINAKA and Yuichiro NAGAME

Advanced Science Research Center, Japan Atomic Energy Research Institute,
Tokai-mura, Ibaraki 319-1195, Japan

Since the discovery of nuclear fission a large number of experimental data have been accumulated for various fissioning system. Up to now several attempts¹⁻⁵ have been made to describe and understand fission phenomena. No theoretical models however are able to predict all the fission observations, mass and kinetic energy distributions and so on because of difficulty in describing drastic and dynamic change of nucleus from saddle to scission. The aim of this work is to interpret systematically properties of fragment mass and total kinetic energy distributions in wide range of actinide fission in view of the asymmetric and symmetric mass division modes.

For the symmetric mass division mode in the pre-actinides, the quantitative explanation of properties of mass and total kinetic energy distributions has been successfully achieved in the frame work of a diffusion model representing fluctuation-dissipative dynamics.⁶ In the present work, based on the concept of this model, new empirical formulae are derived not only for the symmetric mass division mode but also the asymmetric mass division mode. The calculation using the empirical formulae works with only three input parameters, mass and atomic number (A, Z) and excitation energy (E_{ex}) of a fissioning nucleus. The results of the calculation are in good agreement with the experimental data in various fissioning systems.

In the symposium we will present some details of the formulation and evaluate the present calculation, comparing with calculations of other models and experimental data.

1. B. D. Wilkins, et al., *Phys. Rev. C* **14**, 1832 (1976).
2. U. Brosa et al., *Phys. Rep.* **197**, 167 (1990).
3. J. Benlliure et al., *Nucl. Phys. A* **628**, 458 (1998).
4. K. -H. Schmit et al. *Nucl. Phys. A* **665**, 221 (2000).
5. M. C. Duijvestijn et al., *Phys. Rev. C* **64**, 014607 (2001).
6. G. D. Adeev et al., *Sov. J. Part. Nucl.* **19**, 529 (1988).

Primary Fragment Mass-Yield Distributions for Mass-Asymmetric Fission Path of Heavy Nuclei

Y. L. Zhao^{1,2,3,6}, I. Nishinaka², Y. Nagame², K. Tsukada²,
K. Sueki³, S. Goto^{2,4}, M. Tanikawa⁵, and H. Nakahara³

¹Institute of High Energy Physics, Chinese Academy of Science, Beijing 100039, China

²Japan Atomic Energy Research Institute, Tokai, Ibaraki 319-1195, Japan

³Tokyo Metropolitan University, Tokyo 192-0397, Japan

⁴Chemistry Department, Niigata University, Niigata, 950-21, Japan

⁵Department of Chemistry, University of Tokyo, Tokyo 113, Japan

⁶RIKEN, Wako-shi, Saitama 351-0198, Japan

To clarify the characteristics of individual deformation paths that are turned out to be able to provide us with key informations for understanding the mechanism of nuclear fission process, we have performed a series of experiments to determine velocity distributions for fission fragments in each of individual mass splits of heavy elements, using a double velocity time-of-flight (TOF) spectrometer consisting of high time-resolution microchannel plates detectors (MCPDs). The nuclear systems including compound nuclei of ²³³Pa, ²³⁹Np, ²⁴⁵Am and ²⁴⁹Bk with varied excitation energies below 20 MeV were presently investigated. The systematic discussions on the variation of properties of fission paths will be given by combining the present results with literature data ranging from the light to heavy actinides.

As results, the primary fragment mass-yield distributions for individual fission paths are constructed based on the TKE(A₁,A₂)-intensities which are obtained from the analysis of fine structures in the observed distributions of TKE events, the deformation parameter together with masses and charges of a fissioning nucleus as well as fragment nuclei are introduced into the analysis function. The probabilities for nuclei choosing independent fission paths and their dependences on entrance parameters are determined. The experimental results revealed the effects of various aspects including the excitation energy, the deformation parameter of the fissioning nucleus, and the nuclear structure parameter of the outgoing fragment on the formation of mass-yield distribution of fission products.

In addition, following new phenomena are reported, including (i) All of the inner wings of mass-yield distributions of the asymmetric fission path are converged to the same "mass-wall" around A=130 (**A130 mass-wall**); (ii) All of the mass-yield distributions pass through the similar mass position of A_H=144~146 (**A144~146 mass-crossing**); (iii) All of the mass-yield distributions converge to the same position at the fragment mass of A~80 (**A80 mass-convergence**); (iv) The outer wings of the heavier asymmetric mass-yield distributions (on the right hand side) go up with the increase of the fissioning mass A_f (**Rising heavy mass-wing**). These results give out a physical picture showing the formation mechanism of the primary fragment mass-yield distribution in nuclear fission process.

References:

- (1) Y. L. Zhao, et al., Phys. Rev. C62, 014612 (2000); Phys. Rev. Lett. 82, 3408-3411 (1999).
- (2) Y. Nagame, et al., Phys. Lett., B387, 26 (1996); Radiochim. Acta, 78, 3 (1997).
- (3) I. Nishinaka, et al., Proceedings of INPC 2001, Berkeley, Univ. of California, July 30, (2001).
- (4) P. Moller, et al., Nature (London), 409, 785 (2001).

Characteristics of Asymmetric Mass Distributions in Proton-Induced Fission of Actinides

S. Goto¹, D. Kaji¹, I. Nishinaka², Y. Nagame², S. Ichikawa², K. Tsukada², M. Asai², H. Haba², S. Mitsuoka², K. Nishio², M. Sakama³, Y. L. Zhao^{3,4}, K. Sueki³, K. Tanikawa⁵, K. Takamiya⁶, H. Kudo¹, and H. Nakahara³

¹Department of Chemistry, Niigata University, Niigata 950-2181, Japan

²Japan Atomic Energy Research Institute, Tokai, Ibaraki 319-1195, Japan

³Department of Chemistry, Tokyo Metropolitan University, Hachioji, Tokyo 192-0397, Japan

⁴Institute of High Energy Physics, Chinese Academy of Science, Beijing 100039, China

⁵Department of Chemistry, The University of Tokyo, Bunkyo-ku, Tokyo 113-0033, Japan

⁶Research Reactor Institute, Kyoto University, Kumatori, Kyoto 590-0494, Japan

The mass division in the low-energy fissions of light actinides are asymmetric in general. In order to understand this phenomenon, the detailed analyses with respect to the mass distributions in proton-induced fissions of ^{232}Th , ^{238}U , ^{244}Pu , and ^{248}Cm have been carried out¹. As a result, it was found that the lighter side of the heavier fragment mass distribution converges on $A = 126\text{--}128$, while the distributions broadens at the heavier side with the mass number of fissioning nucleus. These features of the asymmetric mass distribution would be caused by the shell structure of the fragments, heavy fragments with $Z = 50$ and complementary light fragments with $N = 50$. Because the fragment mass numbers corresponding to $Z = 50$ and $N = 50$ will change in the systems with different neutron-to-proton ratios (N/Z) of fissioning nuclei, it is expected that the features of asymmetric mass distributions will become different from those in the above systems. In present work, to ascertain this feature, fragment mass and total kinetic energy distributions in proton-induced fissions of uranium isotopes, $^{233,235,238}\text{U}$ ($N/Z = 1.52, 1.54, 1.57$), and plutonium isotopes, $^{239,242,244}\text{Pu}$ ($N/Z = 1.53, 1.56, 1.58$), are precisely measured by the double time-of-flight (TOF) method.

From the measured velocities of two complementary fragments, mass and the total kinetic energy (TKE) of each fragment was determined. The mass distributions were decomposed into the two components, symmetric and asymmetric mass division, by the two component analysis of the TKE distributions¹. In Fig.1, the decomposed distributions of heavy fragments in the 13-MeV proton-induced fission of uranium isotopes are shown. It is found that the lighter side of the distribution shifts to heavier mass number with the fissioning nucleus N/Z as expected.

1. Y. L. Zhao *et al.*, *Phys. Rev. Lett.*, **82**, 3408(1999).

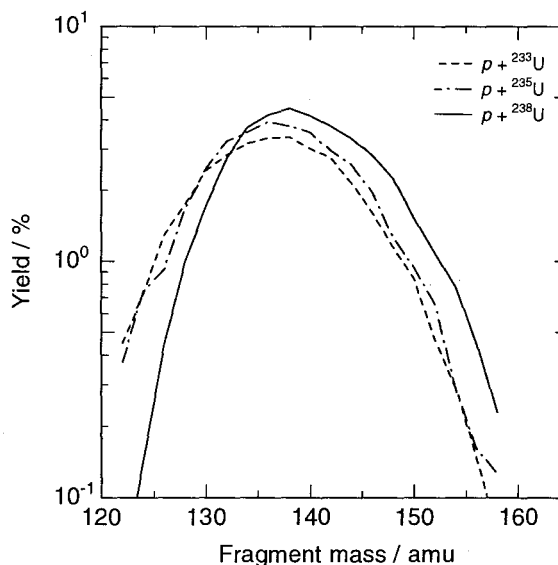


Fig. 1. Heavy asymmetric mass distributions of the 13 MeV $p + ^{233,235,238}\text{U}$ systems.

D. Kaji^{1,2}, K. Morita¹, K. Morimoto¹, Y. L. Zhao^{1,3}, A. Yoneda¹, T. Suda¹, A. Yoshida¹,
H. Kudo², K. Katori¹, and I. Tanihata¹

¹ RIKEN (The Institute of Physical and Chemical Research), 2-1, Hirosawa, Wako-shi, Saitama 351-0198, Japan

² Department of Chemistry, Niigata University, 2-8050, Ikarashi, Niigata 950-2181, Japan

³ Institute of High Energy Physics, Chinese Academy of Science, Beijing P.O.Box918, China

In 2001, a gas-filled type recoil separator (GARIS) has installed at an experimental hall of RIKEN Linear Accelerator (RILAC) facility. The separator was designed for fast (in-flight) and effective collection of the fusion reaction products, separating them from a primary beam. Using the separator with high intensity heavy ion beams (>1 particle μA) from RILAC, we plan to search for new isotopes, including those of new elements whose atomic number is greater than 113. The present setup of GARIS is shown in Fig.1. The separator consists of four magnets in a D_1 - Q_1 - Q_2 - D_2 configuration, where D and Q denote the dipole and quadrupole magnet. A D_2 -magnet is newly added to the system [1] for making a low background condition at high beam intensity.

We will start test experiments to study characteristics of the separator from October 2001. The efficiency of GARIS will be measured with the already-known reaction, such as $^{208}\text{Pb}(^{40}\text{Ar}, 2\text{-}3\text{n})^{246-245}\text{Fm}$. We will also measure the equilibrium charge states of known heavy elements ($Z \geq 108$) in the helium gas. Because it is important to estimate an equilibrium charge state of the heaviest element in helium gas in order to make a proper setup of the separator.

In this report, we present the status of heavy element synthesis in RIKEN.

[1] K. Morita et al., Nucl. Instr. and Meth. **B70**, 220 (1992)

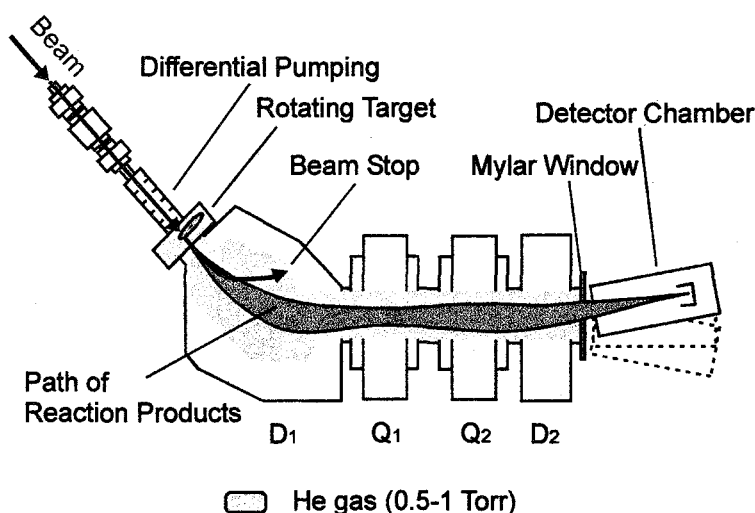


Fig.1 Schematic representation of a gas-filled recoil separator (GARIS)

Radiation-Induced Luminescence and Hydrogen Radical Formation Associated with Thermal Annealing Treatments on White Minerals

Tetsuo HASHIMOTO, Emiko NISHIYAMA and Yuji YANAGAWA

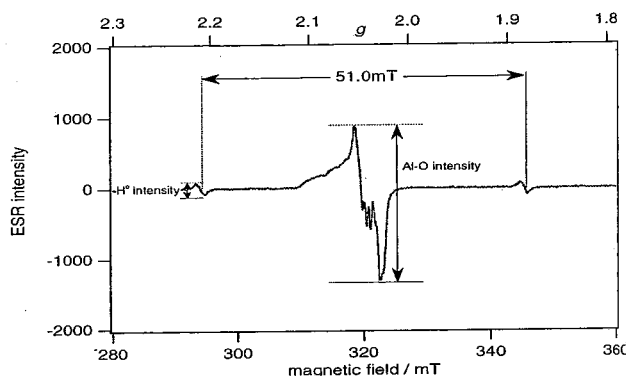
Department of Chemistry, Faculty of Science, Niigata University,
Ikarashi-nincho, Niigata, 950-2181, Japan

1. Radiation-induced luminescence phenomena from natural white minerals, including afterglow (AG) and thermoluminescence (TL), should be related to trapped electrons and positive holes as luminescence centers originating from impurities and/or lattice defects^{1,2)}. An electron spin resonance (ESR) spectrometry, which is well-known to be efficient to investigate the radiation-induced centers such as Al-hole centers, was applied to study hydrogen radical (as one kind of trapped electrons) behavior in the γ -irradiated two kinds of feldspars, associated with thermal treatments. Two new hydrogen radicals emerged in addition to mobile hydrogen radicals after thermal treatment of feldspars.

2 The samples used in this study were selected from museum specimens of natural feldspars. They were chosen from alkali feldspars, that is K- (microcline) or Na-rich (albite) feldspars. Two kinds of feldspar grains (150-250mm diameter) were subjected to the thermal annealing treatments for 30 hours in respectively fixed temperatures, followed to the ESR-spectrometry after gamma-ray irradiation in liquid nitrogen temperature. The samples were irradiated with γ -ray and stored in 77K, followed to ESR spectrometry (using JOEL JES-TE 200).to investigate luminescent centers related to BTL (blue thermoluminescence).

3. Figure 1 illustrates a typical example of ESR spectra for an original albite, which was irradiated at liquid nitrogen temperature following by ESR measurement at the same temperature. In this figure, two kinds of signal, such as Al-O center and hydrogen radicals (H^0), can be observed. Both of them are decayed with intense luminescent emission when warmed up to room temperature. As a result, the Al-O-Al centers together with rapid disappearance of H^0 , which were measured in re-cooling condition. This center could be assigned to a main center of BTL emission.

Unexpectedly, hydrogen radicals trapped in two new sites were observed in addition to an ordinary hydrogen radical site beyond 700 °C annealing treatments. These newly formed hydrogen radicals were found to be relatively stable even in the room temperature and could operate as an Al-hole killer.



1) Hashimoto *et al.* Radiat. Measur. **27**, 243(1997). Fig.1 Typical ESR-spectrum from original albite grains irradiated and measured at 77K.
2) Hashimoto *et al.*, *idem.*, **33**, 429 (2001).

New Aspects of Time Interval Analysis method for the Determination of Artificial Alpha Nuclides

Yasuhiro UEZU^{*1}, Tetsuo HASHIMOTO^{*2}

¹ Japan Nuclear Cycle Development Institute Tokai works, 319-1194 Japan

² Niigata University, 950-2181 Japan

A new determination equipment combined with the time interval analysis (TIA)^{1,2,3} has been developed for the simultaneous determination of concomitant alpha emitting nuclides such as Pu, Am, Cm and natural alpha emitters in dust samples. This discrimination technique for the determination of artificial alpha nuclides is based on the selective subtraction of natural alpha nuclides contribution to total pulses using the time interval distributions of the successive alpha and beta decay events within millisecond or microsecond orders.

The system composes of a Silicon Lithium detector (EURISYS LEC 2000), an amplifier, an analog to digital converter, a multi channel analyzer (Laboratory equipment, List Adapter LN-9100-2M), a timer (Laboratory equipment, Time List LN-9000T) and a personal computer (IBM, Aptiva). The detector is known to offer a high energy-resolution (less than 30 keV at 5.5 MeV) on alpha ray spectrometry. Alpha and Beta pulses can be realized to discriminate within 1 microsecond with this system.

The alpha and beta pulses measured in the SiLi detector are sent to the analog to digital converter and followed to both timing data analyzing and energy data processing circuits and registered into hard disk memories. After counting, these information are drawn, calculated of each time interval and subtracted background events such as natural uranium and thorium progenies from total counting.

Yasuhiro Uezu

Radiation Protection Division, Tokai Works, Japan Nuclear Cycle Development
Institute

4-33 Muramatsu, Tokai-mura, Ibaraki 319-1194, JAPAN

1. T. Hashimoto, M. Noguchi, H. Washio, Y. Yoneyama and Y. Uezu, *J. Radioanal. Nucl. Chem.*, **159**, 2, (1992)
2. T. Hashimoto, Y. Uezu, F. Ishizuka and H. Washio, *J. Radioanal. Nucl. Chem.*, **173**, 1, (1993)
3. T. Hashimoto, Y. Komatsu, D. G. Hong and Y. Uezu, *Radiat. Meas.* **33**, (2001)

BASIC CHARACTERISTICS OF HOLLOW FILAMENT POLYIMIDE MEMBRANE IN GAS SEPARATION AND ITS APPLICATION TO TRITIUM MONITORS

Shinichi Sasaki¹, Eiko Tega², Asako Shimada², Masashi Akahori², Takenori Suzuki¹,
Kenji Okuno², and Kenjiro Kondo¹

¹Radiation Science Center, KEK, Oho1-1, Tsukuba, Ibaraki 305-0801, Japan

²Faculty of Science, Shizuoka University, 836 Shizuoka, Shizuoka 422-8529, Japan

In the high-energy accelerator facility, various radionuclides are produced in the atmospheric air in the beam-line tunnels by thermal-neutron capture and by spallation reactions. Among such airborne species, gaseous radionuclides such as ^3H , ^{11}C , ^{13}N , ^{15}O , and ^{41}Ar are occasionally released to the atmosphere through the stacks, and especially long-lived ^3H and ^{41}Ar may possibly accumulate in the environment. For preservation of the environment around the accelerators it becomes more important to establish an effective technique for measurements of ^3H and ^{41}Ar , since the direct measurements for them at the stack are disturbed by radiations from coexisting short-lived radionuclides. A method for the real-time and continuous monitoring of ^3H using hollow-filament type polyimide membranes has been proposed and developed by us. A hollow-filament type polyimide membrane is one of the most promising devices, because this type of membrane has high separation efficiency with low cost and the incorporation of it to the practical detection system is feasible due to its simplicity and its compactness.

In the present study, the experiments have been performed using a small membrane module system in order to investigate basic characteristics of the membrane for designing the system of real-time measurements. The permeation of interested gases was observed by changing the pressure at permeant side of the module (P_i) and keeping that at feed side (P_h) constant. The enrichment factors, defined as the ratio of mole fraction of interested gas in permeant side to that at feed side, were measured for hydrogen, deuterium, argon, oxygen and carbone dioxide in nitrogen and in air as a function of differential pressure ($P_h - P_i$). The enrichment factor increases with increasing the differential pressure. The factor for hydrogen becomes large rapidly at the differential pressure more than 1×10^5 Pa and exceeds 22, which is the largest value among the factors of the gases used in the experiment. The factors for deuterium are the same as those of hydrogen within the fluctuation of experimental data (3%). On the other hand, the factor for argon does not show remarkable increments. The permeability of the membrane was also examined by the computer simulation using the cross-flow model. The enrichment factors calculated using the permeant coefficient of plane polyimide membrane are in good agreement with experimental results in all gases used.

The preliminary results obtained so far are presented as well as the design concept for the detector system using the membrane, in the presentation.

1 B6 The Improvement of Distillation Unit for Determination of Environmental Tritiated Water

Shing-Fa Fang, Jeng-Jong Wang, Tzu-Wen Wang and Jih-Hung Chiu
Division of Health Physics, Institute of Nuclear Energy Research,
1000 Wen-Hua Road, Chiaan Village, Lungtan, Taoyuan, Taiwan 325, R.O.C.

The general test methods for determination of environmental tritiated water are based on distillation to achieve a purification object, and then add scintillation cocktail for liquid scintillation counting to analyze the tritium concentration in environmental water. The distillation unit usually needs a long condenser to collect the vapor from the sample. This study tries to design a new type of distillation unit, named EZ distiller here, to make the condense process easily and become more compact. It will be easy-handle, water-save and low cost. A group of ions were spiked to a solution for an experiment to identify the EZ distiller performance. These ions include Sr, Y, Ba, Cs, Cr, Co, Mn, Fe, Ni, and Zr. Their radioactive isotopes may interfere liquid scintillation counting and make the tritium analysis error. The decontamination factors of these ions are above 8000 by the distillation of EZ distiller. The losses caused by distillation for three different tritium concentrations (1034.7, 100.53, 10.26 dpm/ml) are about 2.5%.

Key words: Tritium, EZ distiller, Decontamination Factor

Hideki NARUSHIMA¹, Tsutomu SEKINE¹, Yasushi KINO¹, Hiroshi KUDO¹, Mingzhang LIN², and Yosuke KATSUMURA²

¹ Department of Chemistry, Graduate School of Science, Tohoku University, Sendai 980-8578, Japan

² Nuclear Engineering Research Laboratory, School of Engineering, The University of Tokyo, Ibaraki 319-1106, Japan

Technetium(IV) oxide colloids were radiolytically formed by γ irradiation of aqueous solutions of pertechnetate (TcO_4^-), and the formation mechanisms are discussed. Pertechnetate solutions ($5.5 \times 10^{-5} - 2.9 \times 10^{-4} \text{ M}$) were irradiated with bremsstrahlung from an electron linear accelerator at 40 and $17 \pm 3^\circ \text{C}$. The color of the irradiated solutions gradually changed to brownish black, suggesting the formation of Tc(IV) oxide colloids ($\text{TcO}_2 \cdot n\text{H}_2\text{O}$). A transmission electron microscopy (TEM) analysis showed that the size of colloids distributed the range of 30 to 130 nm in diameter. The characteristic X rays from technetium and oxygen were simultaneously detected from colloid particles at the TEM measurements. Round-shaped colloids were produced by the irradiation at 40°C , whereas irregular-shaped colloid particles composed of tiny particles (2 nm in diameter) were produced at 17°C . The concentration of TcO_4^- in the target solutions gradually decreased with an increase of the absorbed dose, corresponding to an increase of the colloid yield. The TcO_4^- fraction sharply decreased in the solution (in the presence of $0.2 \text{ M } t\text{-butyl alcohol}$) deaerated by Ar bubbling before irradiation, but strongly suppressed in the solution saturated with oxygen (O_2) or nitrous oxide (N_2O) gas, as shown in Fig.1. The fact suggests that hydrated electrons play an important role in the course of the reduction of TcO_4^- and that Tc(IV) oxide colloid is formed via successive disproportionation reactions of Tc(VI) and Tc(V).

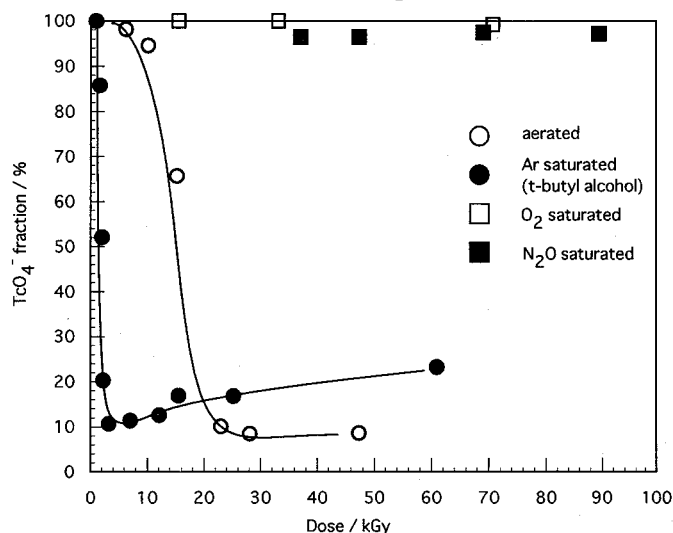


Fig.1 Decrease of TcO_4^- fraction by the bremsstrahlung irradiation for different conditions of the target. Initial concentration of TcO_4^- is 0.1 mM . Irradiation temperature : $17 \pm 3^\circ \text{C}$.

SUBSTITUENT EFFECT ON REDOX POTENTIAL OF NITRIDO TECHNETIUM COMPLEXES WITH SCHIFF BASE LIGAND : THEORETICAL CALCULATIONS

Tsutomu TAKAYAMA, Tsutomu SEKINE and Hiroshi KUDO

Department of Chemistry, Graduate School of Science, Tohoku University, Sendai 980-8578, Japan

We have measured redox potentials between the Tc(V) and Tc(VI) oxidation states of technetium nitrido complexes of [TcN(L)] (L : the salen type Schiff base ligands shown in Fig. 1). The redox potential of [TcN(L1)] with electron withdrawing substituents was higher than that of [TcN(L2)]. On the contrary, the redox potentials of [TcN(L3)] and [TcN(L4)] with electron donating substituents were lower than that of [TcN(L2)]. To understand the experimental results, theoretical calculations were performed in the present work. Theoretical calculations based on the density functional theory were performed by using the Gaussian 94 program. Geometries were optimized with the Becke's three parameter hybrid method using the Lee-Yang-Parr correlation functional (B3LYP). The basis sets are 3-21G for all atoms of the complexes.

Optimized structures of all of these complexes are square pyramidal; *i.e.* two nitrogen atoms and two oxygen atoms of the salen type ligand are in the equatorial plane and the nitrido ligand is at the apical position. The calculated HOMO energies of each complex are plotted against their experimental redox potentials in Fig. 2. The [TcN(L1)] complex has the HOMO energy lower than that of [TcN(L2)]. The HOMO energies of [TcN(L3)] and [TcN(L4)] are higher than that of [TcN(L2)]. Calculated charge populations on the technetium atom are +0.757 for [TcN(L1)], +0.719 for [TcN(L2)], +0.715 for [TcN(L3)] and +0.705 for [TcN(L4)]. The redox potential increases with increasing charge on the technetium atom of [TcN(L)] complexes. The result of calculation indicates that the redox potential of the nitrido technetium complexes with salen type ligands is correlated with the HOMO energy as well as the charge population on the technetium atom.

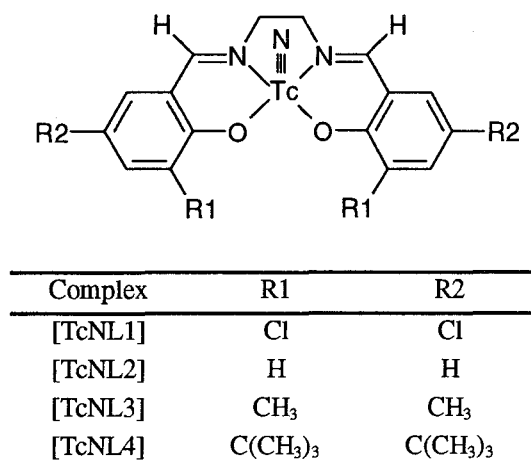


Fig. 1. Structure of complexes for theoretical calculation.

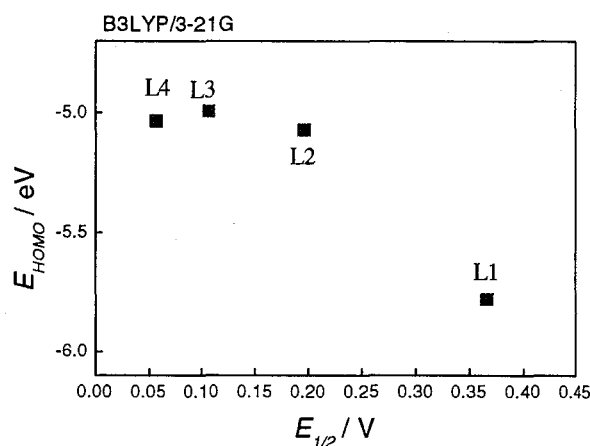


Fig. 2. The plot of the calculated HOMO energy vs. the experimental redox potential of [TcN(L)] (L = L1, L2, L3 and L4).

TECHNETIUM(VII) SULFIDE COLLOID GROWING OBSERVED BY LASER-INDUCED PHOTOACOUSTIC SPECTROSCOPY

Yasushi SAIKI, Masashi FUKUZAKI, Tsutomu SEKINE, Yasushi KINO and Hiroshi KUDO
Department of Chemistry, Graduate School of Science, Tohoku University, Sendai 980-8578,
Japan

Technetium(VII) sulfide colloid growing processes were investigated by laser-induced photoacoustic spectroscopy (LPAS). Technetium(VII) sulfide colloids were prepared by adding aqueous solutions of Na_2S (0.05 M, 0.1 M) to pertechnetate ($^{99}\text{TcO}_4^-$, 0.1 mM) solutions at 25 °C. The color of the solution gradually changed to brown, indicating the formation of sulfide colloids. The yield of colloids, determined by ultrafiltration, increased with increasing reaction time and reached a constant within one day. Analysis of the LPAS signal intensities revealed that the number of colloids in the 0.1 M Na_2S solution was larger than that in the 0.05 M Na_2S solution (Fig. 1), indicating that a larger number of seed particles would be formed in a solution with higher Na_2S concentration. The final particle size of the colloids was 7 nm and 10 nm in diameter in 0.1 M and 0.05 M Na_2S solutions, respectively (Fig. 2). Although the particle size increased at the early stage, the number of the colloid remained constant (Fig. 1). This result suggests that the size of colloid particles increases by deposition of technetium(VII) sulfide on the particle surface, not by coagulation of colloid particles.

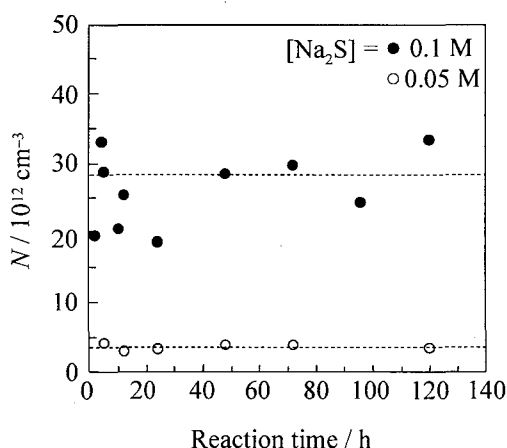


Fig. 1. Time dependence of particle number (N) of Tc_2S_7 colloids per unit volume.

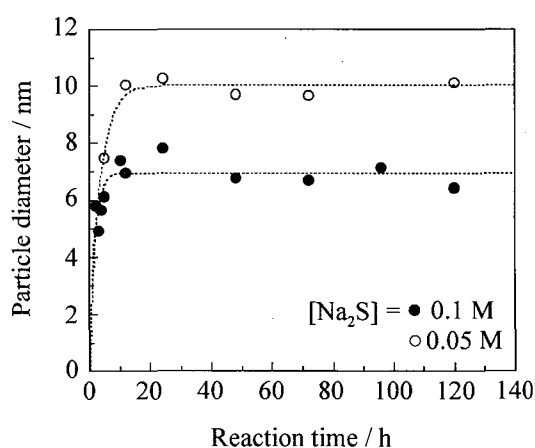


Fig. 2. Time dependence of particle size of Tc_2S_7 colloids.

NON-DESTRUCTIVE DETERMINATION OF TRACE AMOUNTS OF IODINE IN BIOLOGICAL SAMPLES BY EPITHERMAL NEUTRON ACTIVATION AND COMPTON SUPPRESSION GAMMA-RAY SPECTROMETRY

Chushiro YONEZAWA,¹ Hideaki MATSUE¹ and Masae YUKAWA²

¹Japan Atomic Energy Research Institute, Tokai-mura, Naka-gun, Ibaraki-ken 319-1195, Japan; ²National Institute of Radiological Sciences, 4-9-1 Anagawa, Inage-ku, Chiba-shi, Chiba-ken 263-8555, Japan

The importance of iodine in radiation protection, medicinal, nutritional and epidemiological research studies demands an accurate determination of traces of iodine in biological materials. Radioactive nuclides such as ^{38}Cl and ^{24}Na produced from matrices interfere in the trace determination of iodine in biological materials when ^{128}I (half-life 24.99 min) is applied for NAA of iodine. The interference, however, can be reduced by employing epithermal activation and Compton suppression γ -ray spectrometry because the resonance integral of iodine is larger than those of Cl and Na, and the emitting γ -ray energy of ^{128}I is lower than those of ^{38}Cl and ^{24}Na . In the present study, epithermal neutron activation analysis in conjunction with Compton suppression spectrometry has been examined for the determination of iodine in various biological samples.

A sample was irradiated at JRR-4 pneumatic tube using Cd filter for 10 s to 5 min together with an iodine standard. The γ -ray spectra were measured by a Compton suppression spectrometer using a Ge-BGO detector system.

When compared with the case of thermal neutron activation, radioactivities of ^{38}Cl and ^{24}Na induced by the epithermal neutron activation using Cd filter at JRR-4 PN irradiation facility decreased by factors 8.5 and 7.0, respectively, however, the induced radioactivity of ^{128}I decreased by only factor 1.8. The Compton background counts at ^{128}I 443 keV region suppressed by factors 4.3, and 11 for ^{38}Cl and ^{24}Na , respectively, by the Compton suppression γ -ray spectrometry compared to the single mode γ -ray measurement. The detection limits of iodine in biological samples by 1) conventional thermal neutron activation and normal γ -ray measurement, 2) epithermal activation and normal γ -ray measurement, and 3) epithermal activation and the Compton suppression γ -ray measurement were 2600 ppb, 450 ppb and 14 ppb, respectively. More than 35 ppb of iodine in various materials such as human diets, bovine muscle, non-fat milk powder, oyster tissue and human thyroid were determined. The analytical results agreed well with other reported values.

1C2 CORRECTIONS OF NEUTRON SELF-SHIELDING IN ACTIVATION ANALYSIS OF SAMPLES CONTAINING A LARGE AMOUNT OF MANGANESE

Kenji TOMURA and Hiroyuki TOMURO

Institute for Atomic Energy, Rikkyo University
Nagasaka, Yokosuka, 240-0101, Japan

Neutron self-shielding effects on NAA of samples containing a large amount of Mn have been corrected experimentally by varying sample weight stepwise or diluting with water after sample dissolution with HNO_3 and or HF .

No self-shielding effect was observed for iron samples containing a few percent Mn if the sample weight was less than 0.2 g and for ferro- and silicon manganese samples less than 0.02 g. Reliable results can be obtained for ferro- and silicon manganese by repeating the NAA in order to escape from the error caused by sample inhomogeneity.

Empirical formulas were researched to describe the relations between apparent concentration values and sample weights. Better fitness can be attained by a quadratic equation than a linear equation as the function of logarithms of apparent concentration and sample weight. Reliable data can be also obtained from apparent concentrations clearly disturbed by the self-shielding using this quadratic equation.

It was shown that different elements had different self-shielding effects in the same sample by irradiating both cylindrical shaped and thin layered samples mixed the geological reference material of rhyolite with KMnO_4 or KCl . The self-shielding factors were 0.9624, 0.9565 and 0.8949 for ^{24}Na , ^{42}K and ^{56}Mn producing nuclear reactions in the rhyolite sample mixed with KMnO_4 and 0.9008, 0.8542 and 0.9264 for ^{24}Na , ^{42}K and ^{82}Br producing reaction in the sample mixed with KCl . The differences may be explained from that nuclear reactions having giant resonance absorption peaks in epithermal neutron energy range are disturbed strongly by the neutron self-shielding effects.

1 C3 New Technique for Determination of Trace-Elements Using Multiparameter Coincidence Spectrometry

Yuichi Hatsukawa, Yosuke Toh, Masumi Oshima, Taketo Hayakawa,
and Nobuo Shinohara

Japan Atomic Energy Research Institute, Tokai, Ibaraki, 319-1195 Japan

Method of multiparameter coincidence spectrometry based on γ - γ coincidence is widely used in the field of nuclear structure studies, and has produced many successful results. In this study, feasibility of the method of the multiparameter coincidence γ -ray spectrometry for neutron activation analysis was examined.

In the case of neutron activation analysis, measurements of γ -rays from trace elements are strongly interfered by the γ -rays from major elements, e.g., ^{24}Na , ^{56}Mn . So usually chemical separation processes are required to eliminate the major elements for determination of the trace elements. Multiparameter coincidence spectroscopy using 2 Ge detectors was already applied to neutron activation analysis⁽¹⁾. This method, however, has the disadvantage of low efficiency. In this study, to improve the low efficiency of multiparameter coincidence spectrometry, an array of 12 Ge detectors with BGO Compton suppressors was used. Geological and environmental samples were irradiated at JAERI's research reactors with neutron flux $3\text{--}5 \times 10^{13} \text{ ncm}^{-2}\text{s}^{-1}$. Gamma-gamma coincidence of multiple γ -rays from the radioisotopes produced by neutron capture reactions was measured with a array of 12-Ge detectors with BGO Compton suppressors, GEMINI⁽²⁾, located at the tandem accelerator facility in JAERI.

In order to determination of iridium in geological samples, about 100 mg of rock samples were irradiated and γ - γ coincidence measurements were carried out at GEMINI. 20 ppt of iridium was determined without chemical separation. Also long-lived radio isotope, ^{129}I in algae samples were determined. The iodine extracted from algae was precipitated as PbI_2 , and irradiated in JRR-4 reactor. Gamma rays from PbI_2 samples were measured with GEMINI. Contents of ^{129}I are obtained from the intensity of γ - γ coincidence peak from ^{130}I produced by the $^{129}\text{I}(\text{n},\gamma)^{130}\text{I}$ reaction. Detection limit of this method is estimated at $^{129}\text{I}/^{127}\text{I} = 10^{-12}$.

1. G. Meyer, *J. Radioanal. Nucl. Chem.*, 114 223, (1987)

2. K. Furuno, M. Oshima, T. Komatsubara, K. Furutaka, T. Hayakawa, M. Kidera, Y. Hatsukawa, M. Matsuda, S. Mitarai, T. Shizuma, T. Saito, N. Hashimoto, H. Kusakari, M. Sugawara, T. Morikawa, *Nucl. Instr. and Meth. A* **421** 211 (1999)

RADIOACTIVITY MEASUREMENT AND ELEMENT ANALYSIS WITHIN A WOOD DISK BY NEUTRON ACTIVATION ANALYSIS

Y. Hayashi, N. Ikeue, T. M. Nakanishi

*Graduate School of Agricultural and Life Sciences, The University of Tokyo,
1-1-1 Yayoi, Bunkyo-ku, Tokyo, 113-8657*

Summary: Natural radioactivity as well as element profile within wood disks grown both in Indonesia and Japan were measured. The radio-activity of ^{210}Pb was reduced gradually across the disk, suggesting the chronological application of this nuclide. Ca concentration was increased gradually from the center of the disk toward the outer part, whereas Mn and Ca concentration showed reverse tendency.

Key words: annual ring chronology, metasequoia, sugi, wood disk, natural radioactivity, ^{210}Pb , element abundance, neutron activation analysis, Mn, Ca

Since a wood grown in Indonesia does not form an annual ring due to a small change of the climate within a year, the wood disk was analyzed to know the growth and age from the point of radioactivity and element profiles within a wood. First of all metasequoia (*Metasequoia glyptostroboides*) tree cut down in Indonesia was analyzed. The wood disk, which diameter was about 50cm was cut into five pieces and burned to ash. The weight of each fraction of the ash was ranged from 30mg to 60mg. The natural radioactivity, targeting ^{210}Pb , half-life: 22.3y, across the disk was measured by a low background pure Ge counter. It took about a week for each sample to measure ^{210}Pb activity. The 46.5keV of gamma-ray activity emitted from ^{210}Pb was gradually reduced from 0.00467cpm/g to 0.00359cpm/g across the disk, suggesting the chronological application of this nuclide. To measure element profile within a disk, neutron activation analysis was performed. About 100 mg of the disk sample along with the diameter was prepared in a ultra-pure vinyl bag and was irradiated for 5 seconds by a research reactor, JRR-3M, PN-1, installed at Japan Atomic Energy Research Institute, which thermal neutron flux was $5.2 \times 10^{17} \text{ n/cm}^2/\text{s}$. Calcium concentration was increased gradually from the center of the disk toward the outer part, whereas Mn and Ca concentration showed reverse tendency. To compare the data of Indonesian wood with that of Japanese one, Sugi (*Cryptomeria japonica*) was cut down and the wood disk sample was prepared in the same way to measure ^{210}Pb activity and element profiles along with the annual ring.

FAX: +81-3-5841-8193, Email: atomoko@mail.ecc.u-tokyo.ac.jp

NEUTRON ACTIVATION ANALYSIS OF TRACE ELEMENTS AT SEDIMENT-WATER INTERFACE IN LAKE BIWA, JAPAN.

Sadao KOJIMA,¹ Tadashi SAITO,² Jitsuya TAKADA,³ Michikaki FURUKAWA⁴ and
Ki-ichiro YOKOTA⁵

¹Radioisotope Research Center, Aichi Medical University School of Medicine, Nagakute, Aichi-gun, Aichi 480-1195, Japan, ²Radioisotope Research Center, Osaka University, Machikaneyama, Toyonaka 560-0043, Japan, ³Research Reactor Institute, Kyoto University, Kumatori, Sennan-gun, Osaka 590-0494, Japan, ⁴Faculty of Environmental and Information Sciences, Yokkaichi University, Kayo, Yokkaichi 512-8512, Japan and ⁵Lake Biwa Research Institute, Uchidehama, Otsu 520-0806, Japan

Lake Biwa is the widest lake in Japan, and is used by ten million people as a reservoir of drinking, agricultural and industrial water. It is important to determine contents of chemical elements and oxidation states of metal ions at the sediment-water interface in order to reveal the relation of eutrophication of the lake to reduction-oxidation potential in the lake water.

Sediment core samples were collected at the northern part and the southern part of Lake Biwa in various seasons. The collected samples were immediately sliced into a thickness of 0.5-2 cm, and the pore water samples were separated from the sediment samples by centrifugation under oxygen-free conditions on board Hakken-go, Lake Biwa Research Institute. After vacuum freeze-drying, concentrations of Na, Sc, Mn, Fe, As and Sb in the pore water, the bottom water and the sediment were determined by instrumental neutron activation analysis (INAA) at Kyoto University Reactor.

We found that the concentrations of As in the pore water were increasing with the depth in the sediment core. However, the concentrations of Sb in the pore water as well as Na are nearly constant between the sediment surface and 20 cm deep. The behaviors of Sb differ from those of As in the sediment core, though Sb and As belong to the same group on the periodic table. Our previous studies revealed that the concentrations of Mn and Fe in the pore waters, and the ratios of Fe²⁺ to total Fe in the sediments were higher in deep sediment core under the anoxic conditions.¹⁾ The vertical profiles of concentrations of As are similar to those of concentrations of Fe and Mn. The behaviors of the elements at the sediment-water interface in the lake are related to oxidation states of the elements. Phosphorus, one of the most important nutrients, is considered to release from the sediment to the pore water with ferrous ions under the anoxic conditions. We are undertaking the determination of concentrations of P at the sediment-water interface for obtaining the relation of the eutrophication to the reduction-oxidation potential.

1. S. Kojima, M. Furukawa, Y. Sakai, K. Ohshita, H. Oda, T. Nakamura, K. Yokota and M. Yamamoto, in *Environmental Radiochemical Analysis*, G. W. A. Newton (Ed.), The Royal Society of Chemistry, Cambridge(1999) pp. 394-404.

1C6 ACCURACY OF k_0 -FACTORS FOR MULTIELEMENT DETERMINATION BY NEUTRON INDUCED PROMPT GAMMA-RAY ANALYSIS

Hideaki MATSUE, Chushiro YONEZAWA

Department of Environmental Sciences, Japan Atomic Energy Research Institute, Tokai-mura, Naka-gun, Ibaraki-ken 319-1195, Japan

The k_0 standardization method has been studied at JAERI to determine multielements accurately by neutron-induced prompt gamma-ray analysis. So far, the k_0 -factors for 27 elements using Cl as a comparator have been measured with the cold and thermal neutron guided beams of JRR-3M¹. In the present study, we evaluated the accuracy of the present k_0 factors by comparison with: 1) those obtained at the Institute of Isotope and Surface Chemistry (IKI) in Hungary by the use of thermal neutron guided beam², 2) the calculated values from the evaluated data of thermal neutron capture gamma-ray (<http://isotopes.lbl.gov/isotopes/ng.html>), and 3) the analytical results, which were obtained by the k_0 standardization using the present k_0 factors, of various reference materials with certified values. The accuracy of the present k_0 factors is confirmed to be 10% except for Cd and Sm (Fig. 1). The k_0 factor for C showed a tendency to become larger with increasing hydrogen contents in the samples. The k_0 factors for the non-1/v elements such as Cd and Sm varied largely with neutron spectra used for the measurements, because of their large capture cross-sections at relatively low energy region. The effect of difference in neutron spectrum for the non-1/v elements was corrected numerically using neutron spectrum of the beams and neutron cross-section distribution of the elements.

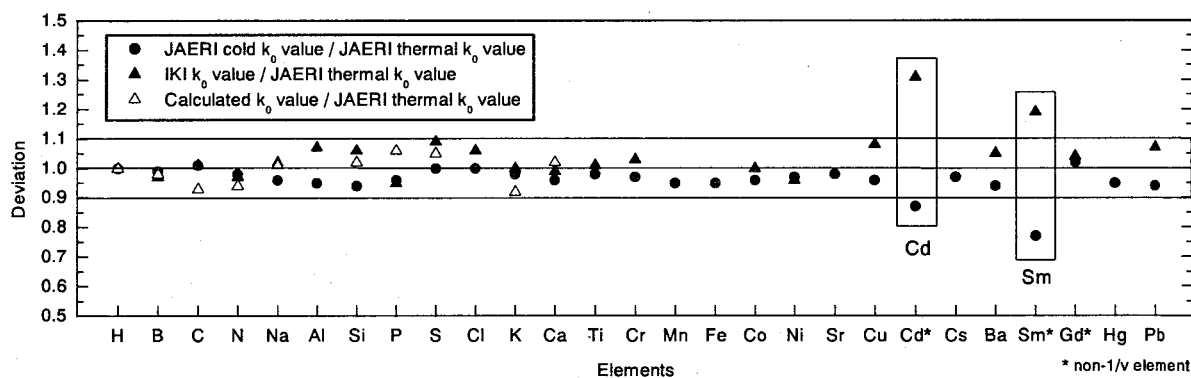


Fig. 1 Comparisons of the k_0 factors among different guided beams and calculated values.

1. H. Matsue, C. Yonezawa, J. Radioanal. Nucl. Chem., **245**(2000) 189.
2. Zs. Révay, G. L. Molnár, T. Belgia, Zs. Kasztovszky, R.B. Firestone J. Radioanal. Nucl. Chem., **244** (2000) 383.

Determination of all platinum-group elements in mantle-derived xenoliths by neutron activation analysis with NiS fire-assay preconcentration

X. L. Li^{1,2}, M. Ebihara¹

¹ Department of Chemistry, Graduate School of Science, Tokyo Metropolitan University, Tokyo 192-0397, Japan

² Shanghai Institute of Nuclear Research, Chinese Academy of Sciences, Shanghai, China

The abundance of platinum-group elements (PGEs) in the earth's upper mantle is of great interest because these data provide important constraints for several fundamental planetary problems. At present, however, only a limited amount of high-quality data is available for PGEs in the earth's upper mantle. This is particularly true for many types of mantle samples where PGE concentrations are typically in the ppb to ppt concentration range. To investigate PGE abundances in the earth's upper mantle, therefore, a modified NiS fire-assay neutron activation method is developed for the determination of all PGEs in mantle-derived xenoliths

The traditional NiS fire-assay procedure has been modified to give lower procedural blanks for PGE analysis. The major modifications are: (1) decrease of nickel powder amounts from 20-30 g to 2 g for a 20 ~ 30 g sample size, and nickel carbonyl powder in place of nickel oxide powder or nickel carbonate powder; (2) use of 6 M HCl in place of 12 M HCl; (3) use of 0.2 μm polytetrafluoroethylene (PTFE) membrane filters in place of 5.0 μm filter papers or 0.45 μm cellulose membrane filters. After these modifications, a lower level blank of < 2 pg/g for Ir, <10 pg/g for Rh, 20 pg/g for Os and <100 pg/g for Ru, Pt and Pd was achieved for a 20 g sample size. Furthermore, previous conditions of instrumental neutron activation analysis (INAA) have been modified to give better detection limits for PGEs. The most significant modification is the use of a higher neutron flux ($4.5 \times 10^{13} \text{ n} \cdot \text{cm}^{-2} \cdot \text{s}^{-1}$) for both long and short irradiations of samples at the JRR-4 reactor of the Japan Atomic Energy Research Institute. Excellent detection limits of INAA for PGEs were obtained: 1 pg/g for Ir, 10 pg/g for Rh, 20 pg/g for Os and 100 pg/g for Ru, Pt and Pd for a 20 g sample size. To obtain analytical data as accurately as possible, interfering reactions and neutron flux gradients and fluctuations are to be carefully considered. The experimental results at JRR-4 show that the neutron flux gradients ($\leq 1\%$ within 2 cm distance) need not be corrected, whereas that the neutron flux fluctuations ($\sim 2.2\%$ at 10 minute's interval, at times) in short irradiations of Rh and the interfering reaction for Pt from Au have to be corrected. The analytical method was evaluated by analyzing the PGE certified rock standard GPt-3. Results of the analyses display an excellent analytical precision (7% ~ 15%) for the ppb concentration PGEs. A good agreement of our results with certified values demonstrates that the analytical method developed in this study is reliable.

The capability of this modified NiS fire-assay neutron activation method for the measurement of PGEs in the upper mantle is illustrated by the exciting results obtained from eastern Chinese peridotite xenoliths. We believe that this method will contribute greatly to PGE mantle geochemistry.

1 C8 Validation of the Accuracy of the LabSOCS Software for Mathematical Efficiency Calibration of Ge Detectors for Typical Laboratory Samples

Frazier L. BRONSON

Canberra Industries, 800 Research Parkway, Meriden CT 06450 USA
tel: 203-639-2345 fax: 203-235-1347 e-mail: fbronson@canberra.com

LabSOCS [Laboratory Sourceless Object Calibration Software] performs mathematical efficiency calibration of Ge detectors. The LabSOCS software is an extension of the ISOCS in-situ product but with improved accuracy for complex shaped sources at close distances, as is common for laboratory users.

Each ISOCS and LabSOCS user receives a "Validation and Internal Consistency" document. This report presents the results of 120 intercomparisons between ISOCS/LabSOCS efficiency calibration and that from a reference method. For laboratory geometries there were 53 tests, with 52 of them using traceable radioactive sources as the reference method. Each test typically had 7-10 energies [about 400 data points for the laboratory sources], and generally covered the energy range from 60-1400 keV. Eight different detectors were used. The difference between the two efficiency values contains contributions from 3 major sources of variability: calibration source inaccuracy, counting statistics, and inaccuracies in the ISOCS/LabSOCS method. The LabSOCS contribution to the total was estimated to be 7.1% sd for energies <150 keV, and 4.3% sd for energies >150 keV.

This process is believed to be an accurate evaluation of the **capability** of the LabSOCS method. However, since this analysis was done on a previous group of detectors, it doesn't tell the user how well his particular detector performs. To help the user answer those questions, a new accessory product ISOXVRFY was created. This product is a report validating the mathematical calibration accuracy for laboratory samples for each individual detector.

Four NIST traceable sources were procured from a reputable commercial laboratory. The geometries for the 4 sources were chosen to represent the range of typical laboratory sources:

- 48mm filter paper; 20cc liquid scintillation vial; 350 cc cylindrical beaker; 2.8 liter Marinelli beaker

Each source contained the following nuclides: Am-241, Cd-109, Co-57, Ce-139, Hg-203, Sn-113, Cs-137, Mn-54, Y-88, Zn-65, and Co-60. This gives 13 well known energy lines for efficiency calibration use, from 60 to 1836 keV. Mn-54 and Zn-65 were added, since 5 of the other energy lines exhibit cascade summing [Y-88, Co-60, and sometimes Ce-139].

All 4 sources were counted on the customer's detector in contact with the endcap. The first 3 were also counted at a distance of 10cm., for a total of 7 different acquisitions. Each of the sources are then modeled with LabSOCS and an energy-efficiency calibration was generated. This LabSOCS calibration was then used to analyzed each of the 7 spectra as an "unknown". The reported results for each energy line was then compared to the "true" decay corrected activity from the source certificate. The ISOXVRFY report is then generated for each customer's detector.

The results from the first 13 detectors produced using this process are summarized here. These sources and counting geometries were deliberately chosen to represent the most difficult calibration geometries for the LabSOCS software. Even so, the results of these new tests were somewhat improved over those published in the "Validation and Internal Consistency" report, especially at low energy. This data shows that efficiency calibrations generated with LabSOCS have improved in accuracy and are now 5.1% sd at low energies and 4.2% sd at high energies.

Hisao Nagai

Department of Chemistry, College of Humanities and Sciences, Nihon University,
Sakura-Josui, Setagaya-ku, Tokyo 156-8550, JAPAN

Cosmogenic nuclides ^7Be (53.4 d) and ^{10}Be (1.5×10^6 yr) are produced in the upper atmosphere, mainly in the stratosphere, by the nuclear reaction of cosmic ray with N and O. These radioactive isotopes are attached to aerosols and carried to the lower troposphere, then they are deposited to the earth's surface mainly by rain. The mean residence time of the aerosols are estimated to 1~2 years and 2~4 weeks in the stratosphere and troposphere, respectively. So, ^{10}Be concentration and $^{10}\text{Be}/^7\text{Be}$ ratio are higher in the stratosphere than those in the troposphere.

Concentrations of cosmogenic nuclides ^7Be and ^{10}Be in rains collected in Tokyo during the last 20 years were determined by γ -ray spectrometry and accelerator mass spectrometry (Fig. 1). For the seasonal variation, the highest values for ^{10}Be flux and $^{10}\text{Be}/^7\text{Be}$ ratio were observed in spring, February to April, and they decreased till the lowest values in autumn. On the other hand, there were not so clear feature for ^7Be flux. These features were caused by the transport of stratospheric air with high ^{10}Be concentration and high $^{10}\text{Be}/^7\text{Be}$ ratio into the troposphere. The annual fluxes for ^7Be and ^{10}Be change cyclic, and the average values for ^7Be and ^{10}Be were ~ 3 and ~ 10 ($\times 10^{-2}$ atom $\text{cm}^{-2} \text{s}^{-1}$) with $\pm 50\%$ and $\pm 30\%$ deviation, respectively. Comparing to the sunspot number as the index of cosmic ray intensity, the annual ^7Be flux was anti-correlated, and also the annual ^{10}Be flux was anti-correlated with two years delay. This implies that the most part of ^7Be and ^{10}Be atoms deposited in Tokyo were produced in the troposphere and stratosphere, respectively.

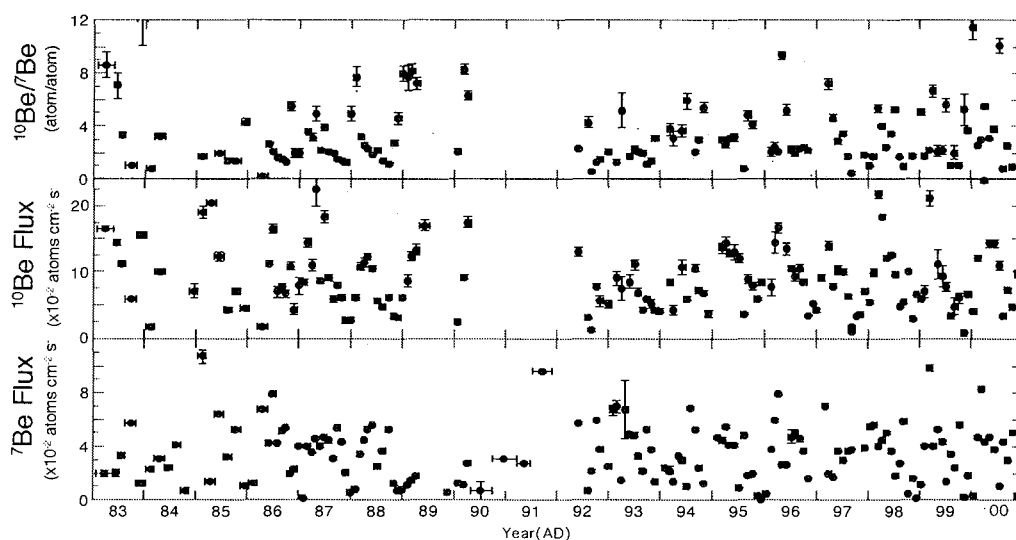


Fig.1 ^7Be and ^{10}Be fluxes and $^{10}\text{Be}/^7\text{Be}$ ratio estimated from the ^7Be and ^{10}Be concentrations in rain collected in Tokyo (1983-2000).

HIGH PRECISION MEASUREMENT OF ^{14}C WITH AMS AND ITS 1 C 10 APPLICATION TO ENVIRONMENTAL STUDIES

Toshio Nakamura¹, Etsuko Niu¹, Hirotaka Oda¹, Tomoko Ohta¹ and Akiko Ikeda¹

¹Center for Chronological Research, Nagoya University, Chikusa-ku, Nagoya-city, 464-8602 Japan

Techniques of accelerator mass spectrometry (AMS), developed since the 1977, based on mainly a tandem accelerator and associated apparatus that are used to analyze charge state, energy, mass number, and atomic number of accelerated ion, enabled us to measure extremely-low abundance (isotope ratio of 10^{-12} to 10^{-16} relative to its stable isotope) nuclides, such as ^{10}Be (half life: 1.5×10^6 yr), ^{14}C (5730 yr), ^{26}Al (7.1×10^5 yr), ^{36}Cl (3.0×10^5 yr), ^{41}Ca (1.0×10^5 yr), ^{129}I (1.57×10^7 yr), etc., in natural samples. Among such nuclides, ^{14}C is the most useful for age determination in archeology as well as a chemical tracer in environmental studies, mainly because carbon is contained by most of archeological remains and environmental chemical substances. The least amount of carbon necessary for AMS ^{14}C measurements has been reduced to about 0.1 mg and the oldest date measurable has been extended to about 50,000-60,000 yr BP, compared to a few grams and about 35,000 yr BP, respectively, for beta-counting measurements of ^{14}C .

A Tandetron AMS system has been used since 1983, to measure ^{14}C concentrations of environmental samples as well as ^{14}C dates of geological and archeological materials, at the Center for Chronological Research (CCR), Nagoya University.^{1,2} We have measured ^{14}C concentrations of more than 8,600 samples from various research fields, for the past 18 years with a GIC Tandetron AMS system. In 1996-1997, we have installed, as a second machine, a new generation Tandetron AMS system which was built by High Voltage Engineering Europe (HVEE), B.V., the Netherlands. We have conducted successfully reproducibility tests of the new machine on the $^{14}\text{C}/^{12}\text{C}$ ratio of better 0.2%, accuracy tests of ^{14}C measurements for IAEA C1 to C8 standard samples, as well as ^{14}C dating of various archeological and geological samples with a precision of less than 0.5%.³

The authors present here a brief review of the present performance, as well as some environmental applications of ^{14}C measurements with the new HVEE Tandetron AMS system of Nagoya University.

1. T. Nakamura, N. Nakai, T. Sakase, M. Kimura, S. Ohishi, M. Taniguchi, and S. Yoshioka, *Jpn. J. Appl. Phys.*, 24, 1716 (1985).
2. T. Nakamura, *The Quaternary Research*, 34(3), 171 (1995).
3. T. Nakamura, E. Niu, H. Oda, A. Ikeda, M. Minami, H. Takahashi, M. Adachi, L. Pals, A. Gottdang, and N. Suja, *Nucl. Instrum and Methods in Physics Research*, B172, 52 (2000).

